Nanotechnology Perceptions
ISSN 1660-6795
www.nano-ntp.com

Numerical Simulation of a Chemo-Fluidic Oscillator with Difference and Finite Element Methods Using P_1 and P_2 Basis Functions in a Taylor-Galerkin Scheme Used in Engineering Applications

Illych Alvarez Alvarez

Escuela Superior Politécnica del Litoral, ialvarez@espol.edu.ec
Universidad Bolivariana del Ecuador, iralvareza@ube.edu.ec

This paper presents a finite element scheme with P1 and P2 basis functions, using an Euler-Taylor-Galerkin method described in [1], for a nonlinear model describing the behavior of a new chemo-fluidic oscillator[2]. This model is expressed by coupling an ordinary differential equation describing the hydrogel dynamics, the equation of nonlinear transport and an auxiliary equation that determines the flow volume. The numerical solution is constructed by taking a semi-discretization in time of the transport equation, employing Taylor series expansions in time forward that includes second and third order derivatives in time, avoiding instability problems. In this semi-discrete equation, the spatial variable is approximated by a finite element formulation according to Galerkin. Some simulations are performed taking different initial conditions for the hydrogel concentration. The numerical results describe the oscillatory behavior of the system as in [2], where the Matlab tools are used as a black box.

Keywords: New Chemo-fluidic Oscillator, Non-linear model, Finite elements, Hydrogel dynamics.

1. Introduction

Autonomous oscillators are a key component of signal processing systems in electronics and biology. The development of oscillators that couple chemical or biological systems with the mechanical domain of microfluids could stimulate novel concepts for the "smart" handling of fluids and their ingredients.

In technology, the realization of chemical oscillators is challenging, unlike electronic

oscillators. Recently, the construction of micro-fluidic oscillators has been demonstrated.

However, these oscillators operate on purely mechanical principles with no influence of the chemical domain on the fluidic domain. In this study, a micro-fluidic oscillator circuit is presented using a chemo-fluidic bulk phase transition transistor and a mixing junction for coupling the chemical and fluidic domains.

This new oscillator operates by constant pressure and flow rate sources without external control signals and generates oscillations of pressure, flow rate and chemical concentration. The oscillator has been shown to have an oscillation period between 200 and 1000 seconds, in addition to chemical concentrations of alcohol ranging from 2wt% (weight percent) to 10wt% and fluid rates in the range of $\mu L\ min^{-1}$.

Chemical oscillations have been first observed by Belousov and Zhabotinsky in the form of chemical oscillation reactions in the 1950s and are a continuing subject of scientific investigations. Yoshida demonstrated that it is possible to investigate the Belousov-Zhabotinsky reaction in a pH-sensitive hydrogel with bulk phase transition behavior and thus couple its expansion and contraction to a chemical reaction system exhibiting pH oscillations.

The oscillator presented here bidirectionally couples the chemical and fluidic domain by means of a chemical volume phase transition transistor (CVPT). CVPTs are based on stimuli-responsive hydrogels. Due to their volumetric phase transition behavior, these materials respond reversibly and reproducibly to small changes of special thermodynamic parameters of the aqueous medium with drastic volume changes any thermodynamic parameter capable of volume elicitation. The phase transition can be the control signal of the oscillator, especially concentrations of organic solvents, ions, ph value or the presence of biomolecules.

Instead, the hydrogel phase transition is stimulated by the change of the alcohol concentration in an aqueous solution. The oscillator employs a microfluidic channel as a delay line for the chemical concentration signal and a CVPT combined with a mixing junction to provide negative feedback. It is interesting to note that nature also uses the approach of a delay and negative feedback in oscillating biochemical systems, and also in modern electronic systems in chips. Delay-based oscillators are ubiquitous in the form of ring oscillators in clock generation and frequency synthesis.

In many aspects of nature, self-oscillating systems play a very important role in the natural sciences (biology or chemistry) as well as in technology (microelectromechanical or electronic systems) and in medicine, because they can be coupled to other systems. One of their most important applications is the use as a system clock to trigger regular events, for example in circadian rhythms or in electronic systems.

This paper deals with the use of a Taylor-Galerkin method for the application of linear finite elements with polynomial basis functions p_1 and p_2; in addition to using and reproducing its numerical modeling by applying finite differences in the time variable to the nonlinear system that controls the behavior of the new chemo-fluidic oscillator and determining its numerical modeling. The mathematical problem was posed by Páez [1] which performed a numerical approximation of the transport PDE using the well-known Line Method. However, the EDOS system provides a very rough approximation of the solution of the equation of the transport.

First, this is due to the first-order discretization in space and, second, because it can propagate abrupt changes or steep fronts, which is a well-known computational problem in the numerical solution of hyperbolic PDEs.

In order to describe the dynamics of the chemo-fluidic oscillator, a set of mathematical models was used, which posed a challenge due to the complexity of the system, since the oscillator is affected by several nonlinearities coming from the hydrogel characteristics and the bidirectional coupling between the chemical and fluidic domains. The hydrogel is designed in such a way that an increase in alcohol concentration reduces its size and vice versa. Therefore, at low alcohol concentrations, the hydrogel valve is closed, while high alcohol concentrations open the valve. A bypass channel is connected to the valve inlet to allow a continuous unidirectional liquid flow near the hydrogel, independent of whether the hydrogel valve is open or closed.

Therefore, to facilitate the modeling process, the system was divided into the fluidic domain, which describes the behavior of the volumetric flows and pressures of the system during operation; and the chemical domain, which in turn was divided into two parts, the description of the hydrogel dynamics and the modeling of the delay line. The latter resulted in a coupled system composed of the EDP of the one-dimensional transport, the EDO that models the dynamic behavior of the hydrogel and the equation that determines the volume in the *buffer*.

We implemented this work on the basis of the work done by Donea [2] who semi-discretizes the equation of nonlinear transport using first, second, and third order Taylor time series expansions to obtain a second order differential equation in space in which the classical variational formulation of Galerkin is applied to obtain a system of linear equations using the finite element method in the spatial variable. This system of linear equations was generated from applying the Euler-Taylor-Galerkin method to the nonlinear transport equation but contains terms that depend on the nonlinear ODE that models the dynamic behavior of the hydrogel. In this case, the variable that determines the size of the hydrogel is $l_v(t)$ which is obtained for each instant of time by applying the Runge-Kutta 4 method, and finally, the volume of the *buffer* that is determined by using numerical integration methods.

Analyzing in much more detail its mathematical modeling and the numerical solution of this new chemical-fluidic oscillator based on smart hydrogels was one of the reasons for the present work. In addition, it is sought to extend the linear method used by Donea [2] for the transport equation to the equation of nonlinear form and provide a solution methodology for new oscillator models involving the one-dimensional nonlinear transport equation.

2. Design of A Chemo-Fluidic Oscillator

The new chemo-fluidic oscillator is based on a negative feedback circuit containing a delay line, where the negative feedback is provided by a hydrogel valve that has the ability to change its size depending on the temperature and the concentration of the aqueous solution that is in direct contact with the hydrogel. In this new oscillator, the temperature is kept constant, so the only parameter that produces a change in the hydrogel size is the alcohol concentration.

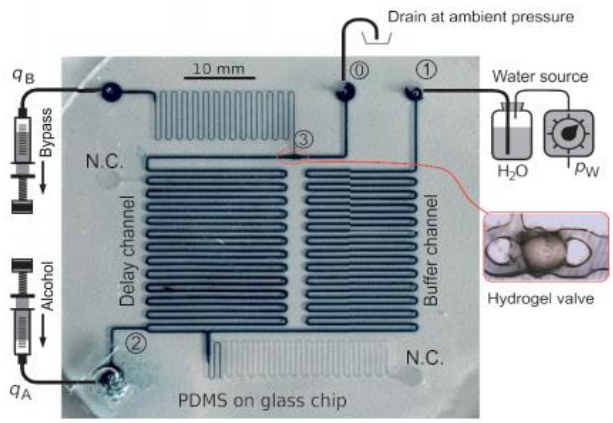

Fig. 1. Photograph of the fabricated chemo-fluidic oscillator circuit, filled with a heavily dyed solution for better visibility of the channels. The external sources of constant flow and pressure are shown schematically. Equivalent fluidic circuit. The hydrogel valve is represented by a controlled flow source.

The oscillator is powered by three constant sources. The first one is a constant flux source q_A supplying the system with a solution of alcohol concentration c_{alc}. A second source provides deionized water at a constant pressure p_W located at node 1. The water flows through a long channel called the buffer line and then mixes at node 2 with the alcohol solution provided by q_A, and then the mixed solution enters the long fluid channel which acts as a delay line. Using this channel, the solution is transported at a rate determined by the flow rate through the delay line $q_2(t)$ and its cross section. The end of this channel is connected to the inlet of the hydrogel valve, whose fluidic behavior is controlled by the alcohol concentration of the solution. Finally, a bypass channel is connected to node 3. to drain the liquid at a constant flow rate q_B suitably chosen.

The micro fluid system will be modeled by means of Kirchhoff's laws within the framework of network theory for a circuit. This approach is used because of the small dimensions of the quantities governing the oscillator operation within the study of micro fluids, since they are in the micro nano and pico liter range. Therefore, pressure is considered analogous to voltage and volumetric flow to electric current, as well as delay lines to resistances. In this context, the oscillator can be described by the fluid network presented in Figure 2.

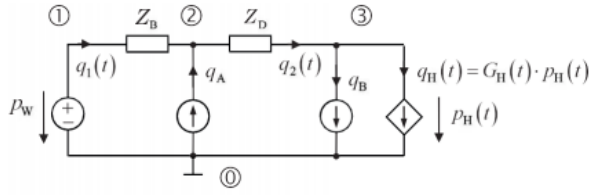

Fig. 2. Equivalent fluidic circuit. The hydrogel valve is represented by a controlled flow source.

3. Mathematical Model of the Chemical-Fluidic Oscillator

The mathematical problem to be studied was posed by Páez et al. in [1], and consists of finding functions l_v: $[0,T] \times [0,1] \to R_+$ such that:

$$\frac{dl_v}{dt}(t) = \gamma[C(t,1)]\{l_{eq}[C(t,1) - l_v(t)]$$
$$l_v(0) = l_v^0$$
$$\Rightarrow \begin{matrix} l_v^0 , C^0(x) = C_{ini}(x) \ \forall x \in (0,1] \\ l_v^{n+1} = F(l_v^n , C^n(1); \Delta t), n = 0,1,2,\dots,N \end{matrix} \qquad (1)$$

$$\frac{\partial C}{\partial t}(t,x) + v\big(l_v(t)\big)\frac{\partial C}{\partial x}(t,x) = 0 \ , \forall (t,x) \in (0,T] \times (0,1] ;$$
$$C(0,x) = C_{ini}(x) , \quad \forall x \in [0, L_d];$$
$$C(t,0) = C_a(t) , \quad \forall t \geq [0,T];$$

(2)

The data in this problem are the functions Υ, l_{eq}, v, C_{ini} , C_a , l_v^0 and where $C(t,1)$ is the unknown value to be determined from the function $C(t,x)$ at the end $x = 1$; which must also be determined simultaneously, in this problem, the function will be determined $V_{buff}(t)$:$[0,T] \to R^+$ defined by:

$$V_{\_vuff}(t) := \int_0^t q_2[l_v(s)]\, ds - q_A t \, ; \forall t \in (0,T], \qquad (3)$$

Where q_2 is a known function and q_A is a constant also known.

A. Semi-discretization in time of the problem (2)

The transport equation is considered as follows

$$\frac{\partial C}{\partial t}(t,x) = -v\big(l_v(t)\big)\frac{\partial C}{\partial x}(t,x) \ , \forall (t,x) \in (0,T] \times (0,1] ;$$

If denoted by $C^n(x)$, the value of the function $C(t,x)$ evaluated in the node $t = t^n$, then a very simple finite-difference scheme to approximate the time derivative in (4) would be the one obtained by the Taylor series expansion, to first order, around point $t^{n+1} = t^n + \Delta t$:

$$C(t^n + \Delta t, x) = C(t^n + \Delta t) + \Delta t \left[\frac{\partial C}{\partial t}\right](t,x)|t = t^n + O(\Delta t)$$

From here, despising the $O(\Delta t)$, the following formula results:

$$\left[\frac{\partial C}{\partial t}\right](t,x) = \frac{C^{n+1}(x) - C^n(x)}{\Delta t}; \qquad (4)$$

which is the well-known forward -time (Euler) type scheme.

If the EDP is now evaluated (4) in $t = t^n$ is available for each $n = 0,1,\dots,N$ the EDO:

$$\left[\frac{\partial C}{\partial t}\right](t,x)|t=t^n = -\left[v[l_v(t)]\right]_{t=t^n}\left[\frac{\partial C}{\partial x}\right](t,x)\Big|_{t=t^n},$$
$$\forall x \in (0,1] \qquad (5)$$

Now, using the forward-time type scheme the expression (5) is transformed into:

$$\frac{C^{n+1}(x)-C^n(x)}{\Delta t} = -v(l_v^n)\frac{\partial C^n}{\partial x}(x), 0 \le n \le N, \forall x \in (0,1] \qquad (6)$$

So, l_v^n is the value of $l_v(t)$ in $t=t^n$ which is determined using Ruge-Kutta 4 applied to the initial problem (1).

Where, in general, $C^n(1)$ is the unknown value $C(t)=1$ on the frontier $x=1$ for the time $t=t^n$. For this scheme, the known constant l_v^0 is the initial iterate. In the context of the finite difference method, the expression (6) produces an unstable numerical scheme when approximating the spatial derivative term using a centered scheme, i.e.:

$$\frac{\partial C^n}{\partial x}(x) = \frac{C_{m+1}^n - C_m^n}{\Delta x} \qquad (7)$$

The instability arises because the partial derivative with respect to the spatial coordinate is evaluated at a time level *n* prior to the time level n where the time derivative term is evaluated. Thus, a stable scheme can be obtained if the two derivative terms $\frac{\partial C}{\partial t}$ and $\frac{\partial C}{\partial x}$ are evaluated at the same time level n (at least to second order in Δt). In this regard, Donea [1] states that the easiest way to make the evaluation of both terms of the expression (6) at the same time level n, is by expressing the difference approximation for the time derivative term at time level n. One way to achieve this is by means of a Taylor series expansion forward in time, including second and third order derivatives. That is, of the expression:

$$C(t^n+\Delta t,x) = C(t^n,x) + \Delta t\left[\frac{\partial C}{\partial x}\right](t,x)\Big|_{t=t^n} + \frac{\Delta t^2}{2}\left[\frac{\partial^2 C}{\partial x^3}\right](t,x)\Big|_{t=t^n} + \frac{\Delta t^3}{6}\left[\frac{\partial^3 C}{\partial x^2}\right](t,x)\Big|_{t=t^n} + O(\Delta t^3) \qquad (8)$$

The term is cleared $\left[\frac{\partial C}{\partial x}\right](t,x)\Big|_{t=t^n}$ and (considering again the notation that was introduced for the forward-time scheme) disregarding the term $O(\Delta t^3)$, and using discretization in time (5), for the equation of transport (4) can be replaced by the following formula:

$$\frac{C^{n+1}(x)-C^n(x)}{\Delta t} - \frac{\Delta t^2}{6}\left[\frac{\partial^3 C}{\partial t^3}\right]^n(x) = -v(l_v^n)\frac{\partial C^n}{\partial x}(x) + \frac{\Delta t}{2}\left[\frac{\partial^2 C^n}{\partial t^2}\right](x), \forall x\,(0,1] \qquad (9)$$

For each $n=0,1,\ldots,N$, the second and third derivative terms appearing in this expression can first be determined by successive differentiation of the equation (4) and then evaluating over time $t=t^n$. The calculation for the second derivative is illustrated below: On one side:

$$\frac{\partial^2 C}{\partial t^2} = v^2 \frac{\partial^2 C}{\partial t^2} - \frac{dv}{dt}\frac{\partial C}{\partial x} \qquad (10)$$

$$\frac{\partial^3 C}{\partial t^3} = v^2 \frac{\partial^2}{\partial t^2} \cdot \left(\frac{\partial C}{\partial t}\right) + 3v \frac{dv}{dt}\left(\frac{\partial^2 C}{\partial x^2}\right) - \frac{\partial C}{\partial x} \cdot \left(\frac{d^2 v}{dt^2}\right) \qquad (11)$$

Now, combining (10) y (11), evaluated in $t = t^n$, with the equation (9), the following formula is the result:

$$\frac{C^{n+1}(x) - C^n(x)}{\Delta t} - \frac{\Delta t^2}{6}\left[v(l_v^n)\frac{\partial^2}{\partial x^2}\left(\frac{\partial C^n}{\partial t}\right)(x) + 3v(l_v^n)\frac{dv(l_v^n)}{dt} \cdot \frac{\partial^2 C^n}{\partial x^2}(x) - \frac{d^2 v(l_v^n)}{dt^2} \cdot \frac{\partial C^n}{\partial x}(x)\right]^1 = -v(l_v^n)\frac{\partial C^n}{\partial x}(x) + \frac{\Delta t}{2}\left[v(l_v^n)\frac{\partial^2 C^n}{\partial t^2}(x) - \frac{dv(l_v^n)}{dt} \cdot \frac{\partial C^n}{\partial x}(x)\right] \qquad (12)$$

$For\ all\ x \in (0\ ,1]\ and\ each\ n = 0,1,\ldots,N$

The expression (12) is similar to the one proposed by Leveque when he generates stabilized numerical methods by adding a diffusive term $\epsilon \frac{\partial^2 C^n}{\partial x^2}$ to the equation of nonlinear transport. However, it should be noted that in (12) the term $\frac{\partial^2 C^n}{\partial x^2}$ appears as part of the difference approximation for the partial derivative of C with respect to time, evaluated at level n. On the other hand, following closely the suggestion of Donea [1], the third order partial derivative term appearing in the Taylor series expansion is purposely expressed in a spatiotemporal mixed form. This mixed form of the derivative will allow the use of finite element type C^0 with a simple modification of the usual and consistent mass matrix in much the same way as is done in the context of weighted Petrov-Galerkin residuals [5].

By developing the specified products and grouping the terms, it is obtained that the problem posed in (11) is semi-discretized in time and for each *n* the following problem is posed,

Given $[0,1] \ni x \ \rightarrow C^0(x) = C_{ini}(x)$, find $C^n(x)_{0 \le n \le N}, \forall x \in [0,1]$, such that:

$$\frac{\partial^2 C^{n+1}(x)}{\partial x^2} - \alpha_1 C^{n+1}(x) = \alpha_2 \frac{\partial^2 C^n(x)}{\partial x^2} + \alpha_3 \frac{\partial C^n(x)}{\partial x} - \alpha_1 C^n(x) \qquad (13)$$

$$\propto_1 = \frac{6}{\Delta t^2 v^2} \ ; \ \alpha_2 = -2 - \frac{3\Delta t}{v}\frac{dv}{dt} \ ; \ \propto_3 = -\frac{\Delta t}{v^2}\frac{d^2 v}{dt^2} - \frac{3}{v^2}\frac{dv}{dt} - \frac{6}{\Delta t v}$$

$$\forall x \in (0,1] \qquad C^n(0) = C_a^n = C_a(t^n)$$

In order to solve the second order differential equation in (15), two conditions are needed, but the problem provides only one condition, so it was necessary to impose a second condition to solve the problem, which is derived from the mathematical model for the self-transport problem of the chemo-fluidic oscillator:

$$\begin{cases} \frac{dl_v}{dt}(t) = \gamma[C(t,1)]\{l_{eq}[C(t,1) - l_v(t)] \\ l_v(0) = l_v^0 \end{cases} \Longrightarrow \begin{matrix} l_v^0 , C^0(x) = C_{ini}(x) \ \forall x \in (0,1] \\ l_v^{n+1} = F(l_v^n , C^n(1); \Delta t), n = 0,1,2, \dots, N \end{matrix}$$

(14)

Condition deduction in $x = 1$

Of the EDP:

$$\mathrm{v}[\mathrm{l_v(t)}]\frac{\partial \mathrm{C}}{\partial \mathrm{x}}(\mathrm{t,x}) = -\frac{\partial \mathrm{C}}{\partial \mathrm{t}}(\mathrm{t,x}) \qquad (15)$$

of semi-discretization of $\frac{\partial C}{\partial t} \Longrightarrow \frac{C^{n+1}(x) - C^n(x)}{\Delta t}$

$$\Rightarrow \mathrm{v}[\mathrm{l_v}(t^{n+1})]\frac{\partial \mathrm{C}}{\partial \mathrm{x}}(t^{n+1},\mathrm{x}) = -\left[\frac{C^{n+1}(x) - C^n(x)}{\Delta t}\right]$$

$$\Rightarrow \mathrm{v}[l_v^{n+1}]\frac{\partial C^{n+1}}{\partial \mathrm{x}}(\mathrm{x}) = -\frac{C^{n+1}(x)}{\Delta t} + \frac{C^n(x)}{\Delta t}$$

$$\Rightarrow \mathrm{v}[l_v^{n+1}]\frac{\partial C^{n+1}}{\partial \mathrm{x}}(\mathrm{x}) + \frac{C^{n+1}(x)}{\Delta t} = \frac{C^n(x)}{\Delta t}$$

(16)

That when evaluated in $x = 1$, a Robin's Condition is obtained.

B. Taylor-Galerkin Method

Considering the domestic product L_2 on the interval $(0,1)$:

$$\langle u, v\rangle_{L_2} := \int_0^1 u(x) \cdot v(x) dx$$

(17)

$$\langle \frac{\partial^2 c_{(x)}^{n+1}}{\partial x^2} - \alpha_1 c_{(x)}^{n+1} - \alpha_2 \frac{\partial^2 c_{(x)}^n}{\partial x^2} + \propto_3 \frac{\partial c_{(x)}^n}{\partial x} - \alpha_1 c_{(x)}^n , v(x)\rangle = 0$$

(18)

Applying the definition of the inner product in the following spaces L_2 , with Dirilecht and Robin boundary conditions, applying the integration by parts formula and replacing the shape functions in (18) for the problem:

$$\begin{matrix} \sum_{j=1}^M c_j^{n+1} \frac{d\varphi_j(1)}{dx}\varphi_i(1) - \sum_{j=1}^M c_j^{n+1} \int_0^1 \frac{d\varphi_j(x)}{dx}\frac{d\varphi_i(x)}{dx} dx \ + \\ \alpha_1 \int_0^1 \left(\sum_{j=1}^M c_j^{n+1}\varphi_j(x)\right) \varphi_i(x) dx \ = -\alpha_2 \sum_{j=1}^M c_j^n \frac{d\varphi_j(1)}{dx}_j \varphi_i(1) \ + \\ \alpha_2 \sum_{j=1}^M c_j^n \int_0^1 \frac{d\varphi_j(x)}{dx}\frac{d\varphi_i(x)}{dx} dx \ + \alpha_3 \sum_{j=1}^M c_j^n \frac{d\varphi_j(x)}{dx}\varphi_i(x) dx \ - \\ \alpha_1 \sum_{j=1}^M c_j^n \int_0^1 \varphi_i(x)\varphi_j(x) dx \qquad \forall \varphi_i, \varphi_j \in V_h \end{matrix} \qquad (19)$$

C. Runge Kutta 4 order method

Initial State $t_1 = 0$

$l_v(t_1) = l_v(1) = l_{ch} = 1.19$

$V_{buff}(t_1) = V_{buff}(1) = 0$

$h(t_1) = h(1) = \frac{1}{2}\big(l_{ch} - l_v(t_1)\big)H\big(l_{ch} - l_v(t_1)\big) = 0$

$L(t_1) = L(1) = 2l_{ch} - h(t_1) - \sqrt{2}w_{dl}$

$G_H(t_1) = G_H(1) = \frac{h(t_1)^3 d_{ch}}{6nL(t_1)}\left(1 - 0.63\frac{h(t_1)}{d_{ch}}\right)$

$q_H(t_1) = q_H(1) = \frac{p_{Eq}G_H(t_1)}{G_H(t_1)Z_{Eq}+1}$

$q_2(t_1) = q_2(1) = q_H(t_1) + q_B$

$q_1(t_1) = q_2(1) = -q_A + q_2(t_1)$

$v(t_1) = v(1) = \frac{q_2(t_1)}{d_{ch}\cdot w_{dl}}$

$c(1;:) = 2{,}26\ (c(x,t)\ for\ x = 1\ is\ at\ the\ end\ of\ the\ delay\ line)$

$l_v'(t) = \Upsilon(c)\left(l_{eq}(c) - l_v(t)\right)$

$\frac{dl_v(t)}{dt} = f(t, l_v)$

$f\big(t, l_v(t)\big) = l_v'(t) = \Upsilon\big(c(k,end)\big)\left(l_{eq}c(k,end) - l_v(t)\right)$

$l_v'(t_k) = \Upsilon\big(c(t_k)\big)\left(l_{eq}\big(c(t_k)\big) - l_v(t_k)\right)$

$k_1 = f(t_k, lv_k) = f\big(t(k), l_v(k)\big) = \gamma\big(c(t_k)\big)\left(l_{eq}\big(c(t_k)\big) - (l_{vk})\right)$

$k_2 = f\left(t_k + \frac{\Delta t}{2}, l_{vk} + \frac{\Delta t}{2}k_1\right) = \gamma\big(c(t_k)\big)\left(l_{eq}\left(c\left(t_k + \frac{\Delta t}{2}\right)\right) - \left(l_{vk} + \Delta t\frac{k_1}{2}\right)\right)$

$k_3 = f\left(t_k + \frac{\Delta t}{2}, l_{vk} + \frac{\Delta t}{2}k_2\right) = \gamma\big(c(t_k)\big)\left(l_{eq}\left(c\left(t_k + \frac{\Delta t}{2}\right)\right) - \left(l_{vk} + \Delta t\frac{k_2}{2}\right)\right)$

$k_4 = f(t_k + \Delta t, l_{vk} + \Delta t) = \gamma\big(c(t_k)\big)\left(l_{eq}\big(c(t_k)\big) - (l_{vk} + \Delta t k_3)\right)$

$l_{vk+1}' = l_v'(t_{k+1}) = l_{vk} + \frac{\Delta t}{6}(k_1 + 2k_2 + 2k_3 + k_4)$

Determining the value of $l_v(t_k)$ for each time instant allows finding the values of each of the system variables for that time instant and feeding these variables into the equation (3.2) discretized in space specifically $\propto_1$, $\propto_2$ y $\propto_3$

$h(t_{k+1}) = \frac{1}{2}\big(l_{ch} - l_v(t_k)\big)H\big(l_{ch} - l_v(t_k)\big)$

$$L(t_{k+1}) = 2l_{ch} - h(t_k) - \sqrt{2}w_{dl}$$

$$G_H(t_{k+1}) = \frac{h(t_k)^3 d_{ch}}{6nL(t_i)}\left(1 - 0.63\frac{h(t_k)}{d_{ch}}\right)$$

$$q_H(t_{k+1}) = \frac{p_{Eq}G_H(t_k)}{G_H(t_k)Z_{Eq}+1}$$

$$q_2(t_{k+1}) = q_H(t_k) + q_B$$

$$q_1(t_{k+1}) = -q_A + q_2(t_k)$$

$$V_{buff}(t_{k+1}) = V_{buff}(t_k) - \left(\frac{q_1(t_{k+1}) - q_1(t_k)}{2}\right)h$$

$$v(t_{k+1}) = \frac{q_2(t_k)}{d_{ch}\cdot w_{dl}}$$

Values of $\propto_1, \propto_2$ and $\propto_3$ in the equation of transport discretized in time using the Euler-Taylor-Galerkin method and then solved in space by applying the finite element method.

$$\propto_1 = \frac{-6}{\mathrm{dt}^2 \cdot \mathrm{v_{(k)}}}$$

$$\propto_2 = -\left(2 + \frac{3\Delta t}{v_{(k)}} \cdot \left(\frac{dv}{dt}\right)\right)$$

$$\propto_3 = -\frac{\Delta t}{v^2}\cdot\frac{d^2v}{dt^2} - \frac{3}{v^2}\frac{dv}{dt} - \frac{6}{\Delta t \cdot v}$$

$$\begin{aligned}
c_i^{n+1}\varphi_{i+1}(1)\frac{d\varphi_i(1)}{dx} &+ c_{i+1}^{n+1}\varphi_{i+1}(1)\frac{d\varphi_{i+1}(1)}{dx} - c_i^{n+1}\int_{x_i}^{x_{i+1}}\frac{d\varphi_{i+1}(x)}{dx}\frac{d\varphi_i(x)}{dx}\,dx \\
&- c_{i+1}^{n+1}\int_{x_i}^{x_{i+1}}\frac{d\varphi_{i+1}(x)}{dx}\frac{d\varphi_{i+1}(x)}{dx}\,dx + \alpha_1 c_i^{n+1}\varphi_{i+1}(x)\varphi_i(x) \\
&+ \alpha_1 c_{i+1}^{n+1}\varphi_{i+1}(x)\varphi_{i+1}(x) \\
&= -\alpha_2 c_i^n\frac{d\varphi_{i+1}(1)}{dx}\varphi_i(1) - \alpha_2 c_{i+1}^n\frac{d\varphi_{i+1}(1)}{dx}\varphi_{i+1}(1) \\
&+ \alpha_2 c_i^n\int_{x_i}^{x_{i+1}}\frac{d\varphi_{i+1}(x)}{dx}\frac{d\varphi_i(x)}{dx}dx + \alpha_2 c_{i+1}^n\int_{x_i}^{x_{i+1}}\frac{d\varphi_{i+1}(x)}{dx}\frac{d\varphi_{i+1}(x)}{dx}dx \\
&+ \alpha_3 c_i^n\int_{x_i}^{x_{i+1}}\varphi_{i+1}\frac{d\varphi_i(x)}{dx}dx + \alpha_3 c_{i+1}^n\int_{x_i}^{x_{i+1}}\varphi_{i+1}\frac{d\varphi_{i+1}(x)}{dx}dx \\
&- \alpha_1 c_i^n\int_{x_i}^{x_{i+1}}\varphi_{i+1}(x)\varphi_i(x)\,dx \\
&- \alpha_1 c_{i+1}^n\int_{x_i}^{x_{i+1}}\varphi_{i+1}(x)\varphi_{i+1}(x)\,dx \qquad \forall\varphi_i, \varphi_j \in V_h
\end{aligned}$$

D. Finite Element Method with Basis Functions P_1

A finite element discretization as explained above, but adapted to the working range, will be considered $[0,1]$. In fact, the partitioning of this interval corresponds to the longitudinal discretization of the delay line channel in $(M-1)$ elements $I_j = [x_j, x_{j+1}]$ in length $h_j = x_{j+1} - x_j$ for $j = 1,2,3,\ldots,M$. Being $h_i = h$, the partition represents a grid of points x_j denoted by τ_h.

By writing (19) using the elementary formulation, the following would be:

$$\begin{bmatrix} \frac{d\varphi_i'(1)}{dx}\cdot\varphi_i(1) & \frac{d\varphi_i'(1)}{dx}\cdot\varphi_{i+1}(1) \\ \frac{d\varphi_{i+1}'(1)}{dx}\cdot\varphi_i(1) & \frac{d\varphi_{i+1}'(1)}{dx}\cdot\varphi_{i+1}(1) \end{bmatrix}\begin{bmatrix} C_i^{n+1} \\ c_{i+1}^{n+1} \end{bmatrix} -$$
$$\begin{bmatrix} \frac{d\varphi_i'(0)}{dx}\cdot\varphi_i(1) & \frac{d\varphi_i'(0)}{dx}\cdot\varphi_{i+1}(1) \\ \frac{d\varphi_{i+1}'(0)}{dx}\cdot\varphi_i(1) & \frac{d\varphi_{i+1}'(0)}{dx}\cdot\varphi_{i+1}(1) \end{bmatrix}\begin{bmatrix} C_i^{n+1} \\ c_{i+1}^{n+1} \end{bmatrix} + \frac{1}{h_i}\begin{bmatrix} 1 & -1 \\ -1 & 1 \end{bmatrix}\begin{bmatrix} C_i^{n+1} \\ c_{i+1}^{n+1} \end{bmatrix} +$$
$$\frac{\alpha_1}{6}h_i\begin{bmatrix} 2 & 1 \\ 1 & 2 \end{bmatrix}\begin{bmatrix} C_i^{n+1} \\ c_{i+1}^{n+1} \end{bmatrix} + \frac{-\propto_{311}}{2}\begin{bmatrix} -1 & 1 \\ -1 & 1 \end{bmatrix}\begin{bmatrix} C_i^{n+1} \\ c_{i+1}^{n+1} \end{bmatrix}[c_M^{n+1}] =$$
$$\propto_2 \begin{bmatrix} \frac{d\varphi_i'(1)}{dx}\cdot\varphi_i(1) & \frac{d\varphi_i'(1)}{dx}\cdot\varphi_{i+1}(1) \\ \frac{d\varphi_{i+1}'(1)}{dx}\cdot\varphi_i(1) & \frac{d\varphi_{i+1}'(1)}{dx}\cdot\varphi_{i+1}(1) \end{bmatrix}\begin{bmatrix} C_i^n \\ c_{i+1}^n \end{bmatrix} -$$
$$\propto_2 \begin{bmatrix} \frac{d\varphi_i'(0)}{dx}\cdot\varphi_i(0) & \frac{d\varphi_i'(0)}{dx}\cdot\varphi_{i+1}(0) \\ \frac{d\varphi_{i+1}'(0)}{dx}\cdot\varphi_i(0) & \frac{d\varphi_{i+1}'(1)}{dx}\cdot\varphi_{i+1}(0) \end{bmatrix}\begin{bmatrix} C_i^n \\ c_{i+1}^n \end{bmatrix} + \frac{-\propto_2}{h_i}\begin{bmatrix} 1 & -1 \\ -1 & 1 \end{bmatrix}\begin{bmatrix} C_i^n \\ c_{i+1}^n \end{bmatrix} +$$
$$\frac{\propto_{322}}{2}\begin{bmatrix} -1 & 1 \\ -1 & 1 \end{bmatrix}\begin{bmatrix} C_i^n \\ c_{i+1}^n \end{bmatrix} + \frac{\propto_1 h_i}{6}\begin{bmatrix} 2 & 1 \\ 1 & 2 \end{bmatrix}\begin{bmatrix} C_i^n \\ c_{i+1}^n \end{bmatrix} \qquad (20)$$

E. Finite Element Method with Basis Functions P_2

In the analysis of this problem, the Delay Line was considered longitudinally, so that polynomials of degree one were used for the shape functions (base) where each element has 2 nodes and the aforementioned results were obtained, but in a search to refine the mesh in the spatial variable using polynomials of a higher order, an element with 3 nodes was used, so that the shape functions are of quadratic type where $\varphi_1(x)$ takes the value of one at the initial node (left end of the element) and cancels out at all other nodes; $\varphi_2(x)$ is the function that takes the value of one at the intermediate node (center of the element) and zero at the other nodes, and $\varphi_3(x)$ which takes the value of one at the end node (right end of the element) and zero at the other nodes. Thus, when performing the analysis for any element, it has the associated nodes $i, i+1, i+2$.

After that, a reference element is defined $\widehat{\Omega}$ with nodes at the ends and in the middle $(\xi_1 = -1\,, \xi_2 = 0\,, \xi_3 = 1\ )$, giving rise to the quadratic basis functions:

$$\widehat{\varphi_1}(\xi) = \frac{1}{2}\xi(\xi-1)\ ,\ \widehat{\varphi_2}(\xi) = (\xi+1)(1-\xi)\ ,\ \widehat{\varphi_3}(\xi) = \frac{1}{2}\xi(\xi+1)$$

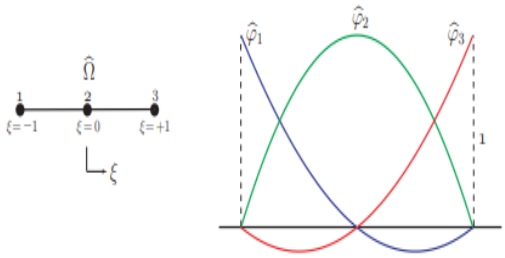

So local basis functions are generated $\varphi_i^{(e)}(x)=\widehat{\varphi_1}(\xi)$, $\varphi_{i+1}^{(e)}(x)=\widehat{\varphi_2}(\xi)$, $\varphi_{i+2}^{(e)}(x)=\widehat{\varphi_3}(\xi)$.

Working with quadratic polynomials generates changes in the elementary formulation because they would no longer be 2x2 matrices, but 3x3 matrices since there are 3 nodes for each element.

The system of equations of the elementary formulation is written taking into account 3 nodes per element.

$$\begin{bmatrix} \frac{d\varphi_i'(1)}{dx}\cdot\varphi_i(1) & \frac{d\varphi_{i+1}'(1)}{dx}\cdot\varphi_i(1) & \frac{d\varphi_{i+2}'(1)}{dx}\cdot\varphi_i(1) \\ \frac{d\varphi_i'(1)}{dx}\cdot\varphi_{i+1}(1) & \frac{d\varphi_{i+1}'(1)}{dx}\cdot\varphi_{i+1}(1) & \frac{d\varphi_{i+2}'(1)}{dx}\cdot\varphi_{i+1}(1) \\ \frac{d\varphi_{i+2}'(1)}{dx}\cdot\varphi_i(1) & \frac{d\varphi_{i+1}'(1)}{dx}\cdot\varphi_{i+2}(1) & \frac{d\varphi_{i+2}'(1)}{dx}\cdot\varphi_{i+2}(1) \end{bmatrix}\begin{bmatrix} C_i^{n+1} \\ C_{i+1}^{n+1} \\ C_{i+2}^{n+1} \end{bmatrix} -$$

$$\frac{1}{3h}\begin{bmatrix} 7 & -8 & 1 \\ -8 & 16 & -8 \\ 1 & -8 & 7 \end{bmatrix}\begin{bmatrix} C_i^{n+1} \\ C_{i+1}^{n+1} \\ C_{i+2}^{n+1} \end{bmatrix} + \frac{\alpha_1}{15h}\begin{bmatrix} 8 & -16 & 8 \\ -16 & 32 & 4 \\ 8 & 4 & 8 \end{bmatrix}\begin{bmatrix} C_i^{n+1} \\ C_{i+1}^{n+1} \\ C_{i+2}^{n+1} \end{bmatrix} -$$

$$\frac{\alpha_{311}}{h}\begin{bmatrix} -\frac{1}{2} & \frac{2}{3} & -\frac{1}{3} \\ -\frac{2}{3} & 0 & \frac{2}{3} \\ \frac{1}{3} & -\frac{2}{3} & 1 \end{bmatrix}\begin{bmatrix} C_i^{n+1} \\ C_{i+1}^{n+1} \\ C_{i+2}^{n+1} \end{bmatrix}[c_M^{n+1}] =$$

$$\propto_2 \begin{bmatrix} \frac{d\varphi_i'(1)}{dx}\cdot\varphi_i(1) & \frac{d\varphi_{i+1}'(1)}{dx}\cdot\varphi_i(1) & \frac{d\varphi_{i+2}'(1)}{dx}\cdot\varphi_i(1) \\ \frac{d\varphi_i'(1)}{dx}\cdot\varphi_{i+1}(1) & \frac{d\varphi_{i+1}'(1)}{dx}\cdot\varphi_{i+1}(1) & \frac{d\varphi_{i+2}'(1)}{dx}\cdot\varphi_{i+1}(1) \\ \frac{d\varphi_{i+2}'(1)}{dx}\cdot\varphi_i(1) & \frac{d\varphi_{i+1}'(1)}{dx}\cdot\varphi_{i+2}(1) & \frac{d\varphi_{i+2}'(1)}{dx}\cdot\varphi_{i+2}(1) \end{bmatrix}\begin{bmatrix} C_i^n \\ C_{i+1}^n \\ C_{i+2}^n \end{bmatrix} -$$

$$\frac{\propto_2}{3h}\begin{bmatrix} 7 & -8 & 1 \\ -8 & 16 & -8 \\ 1 & -8 & 7 \end{bmatrix}\begin{bmatrix} C_i^n \\ C_{i+1}^n \\ C_{i+2}^n \end{bmatrix} + \frac{\propto_{322}}{2h}\begin{bmatrix} -\frac{1}{2} & \frac{2}{3} & -\frac{1}{3} \\ -\frac{2}{3} & 0 & \frac{2}{3} \\ \frac{1}{3} & -\frac{2}{3} & 1 \end{bmatrix}\begin{bmatrix} C_i^n \\ C_{i+1}^n \\ C_{i+2}^n \end{bmatrix} + \frac{\alpha_1}{15h}\begin{bmatrix} 8 & -16 & 8 \\ -16 & 32 & 4 \\ 8 & 4 & 8 \end{bmatrix}\begin{bmatrix} C_i^n \\ C_{i+1}^n \\ C_{i+2}^n \end{bmatrix}$$

4. Numerical Experimentation

After the mathematical part of the model and obtaining the system of equations, a Matlab program was designed for the coupled system where several tests were carried out with their

respective numerical adjustments according to the theoretical definitions explained in chapters 2 and 3.

Each experiment details the change in initial concentration $C(0,x) = c_{ini}(x)$ which is a unique experimental value for hydrogel performance that is not reported in Paez [1] and has been imposed on the basis of the physical model.

A. Experiment 1

The values are taken in the space of $M = 20$ (nodes); $dx = \frac{1}{M-1}$; $Courant = \frac{dt}{dx}$;$dt = Courant \cdot dx$; Courant= 0.1

The following was taken as a condition $C(0,x) = c_{ini}(x)$ a constant value that in this case is the experimental value with which they worked on the numerical part in the initial study $c_{ini}(x) = 2.2635$.

The values of the derivatives of the concentration found in α_3 are replaced by forward differences (Euler) for $t \geq 0$.

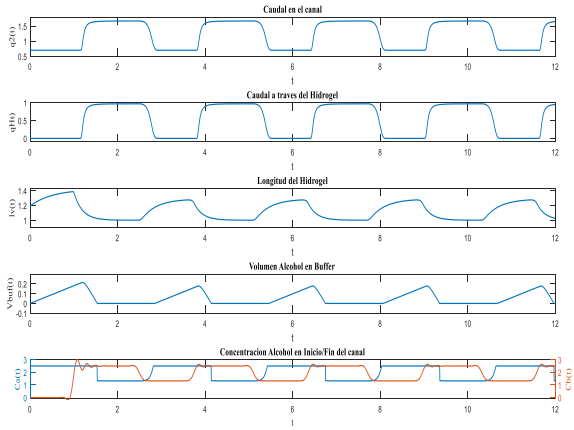

Fig. 3 Response of the chemo-fluidic oscillator modeled by the system.

A periodic behavior can be observed in the hydrogel, which is what allows the device to function as an oscillator with negative feedback due to the increase and decrease of the alcohol mixture in the hydrogel chamber, but at the beginning of the flow of the alcohol and water mixture there is instability in the wave fronts that then regularize as the process of opening and closing the valve progresses because the hydrogel undergoes a deformation greater than the length of the chamber

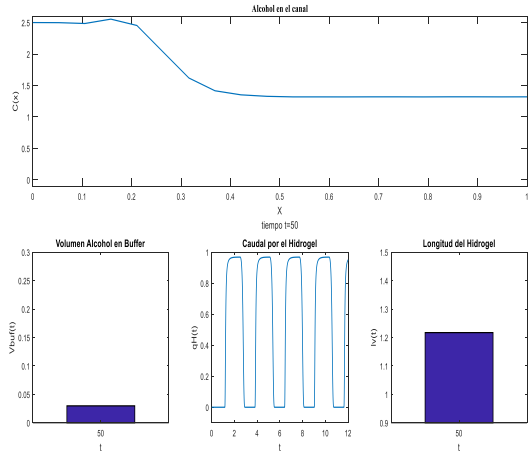

Fig. 4. Response of the chemo-fluidic oscillator modeled by the state variables.

B. Experiment 2

In this test, a quadratic profile was taken as the initial condition, given that in the channel there is a mixture of water and alcohol resulting from the flow of deionized water and alcohol, but it does not reach the minimum concentration level for the hydrogel to react and begin to compress due to the increase in alcohol. There is a periodic behavior, but with less disturbance at the beginning of the process, which allows a more stable and smoother concentration flow in the wave fronts.

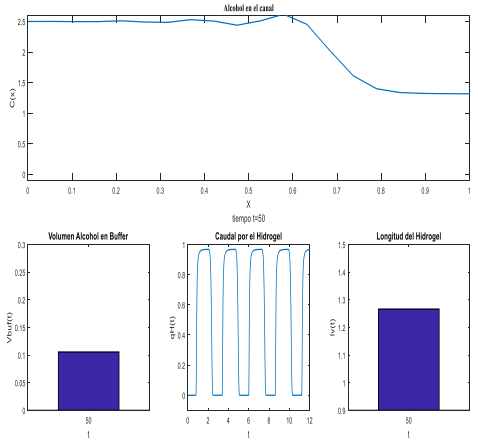

Fig. 5. Response of the chemo-fluidic oscillator modeled by the state variables.

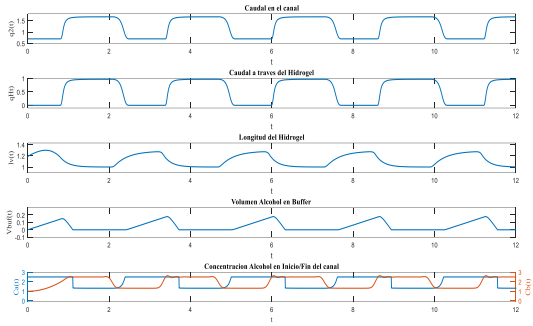

Fig. 6. Response of the chemo-fluidic oscillator modeled by the system.

C. Experiment 3: Graphical Analysis of Methods

1. Graphical Analysis of Methods

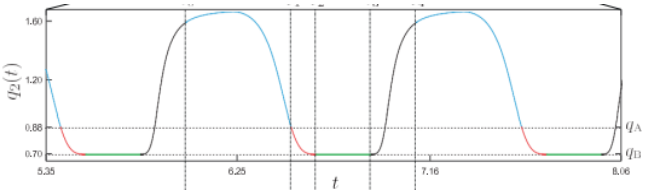

Fig. 7. Results Line Method

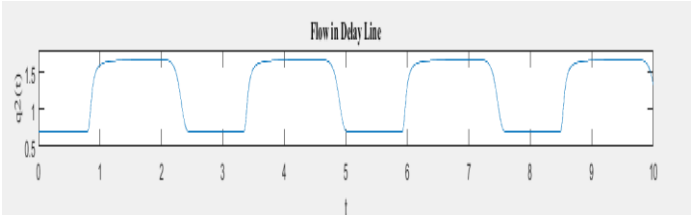

Fig. 8. Results One-dimensional Finite Element Method P_1

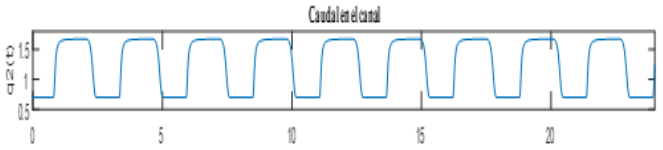

Fig. 9. Results One-dimensional Finite Element Method P_2

2. Volume of alcohol in the Buffer

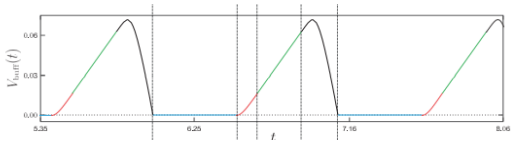

Fig. 10. Results Line Method

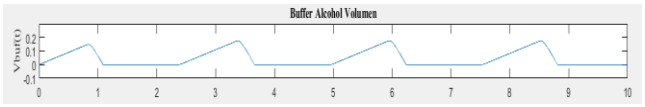

Fig. 11. Resultados Método de Elementos Finitos unidimensional P_1

Fig. 12. Results One-dimensional Finite Element Method P_2

3. Alcohol concentration at the beginning (C_a) and at the end (C_b) of the Delay line

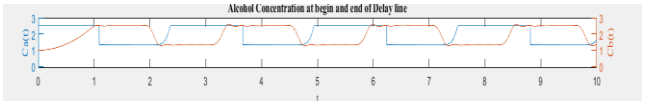

Fig. 13. Results Line Method

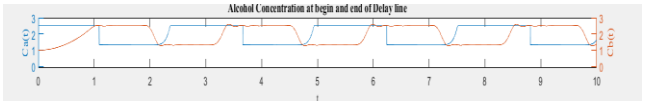

Fig. 14. Result One-dimensional Finite Element Method P_1

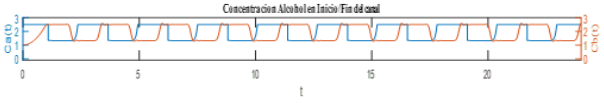

Fig. 15. Result One-dimensional Finite Element Method P_2

4. Hydrogel size behavior during operation.

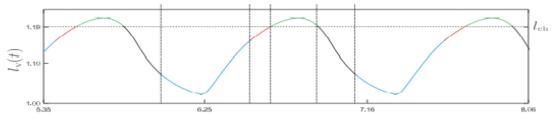

Fig. 16. Results Line Method

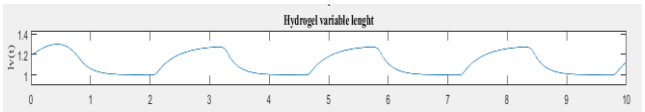

Fig. 17. Results Finite Element Method P_1

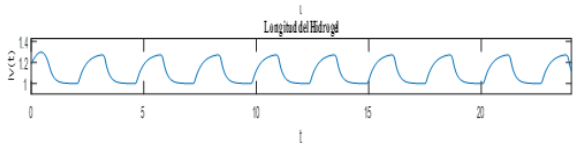

Fig. 18. Results Finite Element Method P_2

5. Conclusions and Recommendations

The first observation that can be made is that the method applied to the system composed of the equations $(15), (16)\ and\ (17)$ reproduces the dynamics of the original Paez Numerical Model [1]. Small differences in amplitude and period are found, but it is able to produce stable periodic signals for the parameter settings without requiring any external forcing, which means that the oscillatory behavior is self-excited.

The second observation is that from a numerical approximation of the equation of linear transport (constant velocity) based on the Euler-Taylor-Galerkin method for the discretization in time and the Finite Element Method for the discretization in space proposed by Donea, by applying the same method with some variations in the initial and boundary conditions in the equation of the transport of the nonlinear system that is also coupled to a nonlinear ordinary differential equation that governs the behavior of the hydrogel and another equation that controls the volume of the buffer giving us as a result a complex system to solve, satisfactory results were obtained in relation to its oscillation and its periodic and bounded motion. It is very important to notice that this numerical model allows to observe that if the C_{ini} initial value is changed, a variation will occur at the beginning of the hydrogel operation, which would be in the stationary regime, but after this initial regime the hydrogel shows an oscillatory and periodic behavior typical of the initial Paez analysis.

The third observation is that this numerical analysis applied to the chemo-fluidic oscillator analytically contributes to the understanding that the hydrogel composite valve is extremely sensitive to parameter variation. That is, it has the ability to drastically change its volume under small variations of special thermodynamic parameters.

When solving the system and plotting the results for 20 nodes (19 elements) in the spatial discretization, it can be observed that the period decreases as a result of the mathematical refinement in space. Therefore, it is very similar to the plots proposed in the initial investigation. It can also be noticed that the small perturbations present in the wavefronts decrease to almost minimum due to the instantaneous deformation of the hydrogel.

In this research, it was possible to give another option to mathematically model the oscillator domains, in the fluidic domain given by the flow network, the transport of the concentration through the delay line; and in the chemical domain, given by the behavior of the hydrogel and the alcohol concentration that produce a smooth dynamic system by parts.

It is recommended to use for future studies a mathematical refinement method, such as the Galerkin-Discontinuous method, in order to model in a more detailed way the behavior of the chemo-fluidic oscillator.

References

1. J. Páez, "Un nuevo oscilador quimio-fluídico autoexcitado basado en Hidrogeles sensibles a estímulos: modelo matemático y comportamiento dinámico," junio 2016.
2. J. Donea, "A Taylor-Galerkin method for convective transport problems," Int. J. for Numerical Methods in Engineering, vol. 20, num. 1, pp. 101-119, enero 1984.
3. P.D. Lax and B. Wendroff, "On the stability of difference schemes," Comm. On Pure Appl. Math., vol. XV, pp. 363-371, 1960.
4. P. D Lax and B. Wendroff, "Difference Schemes for Hyperbolic equations with high order of accuracy," Comm. On Pure Appl. Math., pp. 381-398, 1964.
5. C.E. Leith, Methods in Computational Physics, vol. 4, p. 1, Academic Press, New York, enero 1, 1965.
6. J.K. Dukowicz and J.D. Ramshaw, "Tensor viscosity method for convection in numerical fluid dinamics," J. of comp. physics, vol. 32, pp. 71-79, julio 1979.
7. D. Kuzmin, "Explicit and implicit FEM-FCT algorithms with flux linearization," J. of comp. physics, vol. 228, num. 7, pp. 2517-2534, abril 2009.
8. F. Mesinger , "Forward-back scheme, and its use in a limited area model", Contrib. Atmos. Phys., vol. 50, pp. 200-210, 1977.
9. Courant Number. Introducción a la Simulación de Fluidos Ivan Aldear 2012.
10. "Algoritmo explícito para la ecuación Advetiva en el FTCS" Modelacion Numerica de la Atmosfera 2017. Marcelo Barreiro.
11. A. Lenk, R. G. Ballas, R. Werthschützky, and G. Pfeifer, Electromechanical Systems in Microtechnology and Mechatronics: Electrical, Mechanical and Acoustic Networks, their Interactions and Applications. Springer, 2011.
12. R. R. K. Garg, A. Dixit, and P. Yadav, Basic Electronics, Laxmi Publications, 2009.
13. A. Richter, J. Wenzel, and K. Kristchmer, "Mechanically adjustable chemostats based on Stimulli-Responsive polymers," Sensor Actuat .B Chem., vol. 125, no. 2, pp. 569-573, 2007.
14. K. W. Morton, and A. K. Parrott, "Generalised Galerkin methods for first-order hyperbolic equations," J. of Compt. Phys. 36, pp. 249-270, July 1980.
15. J. K. Dukowics, and J. D. Ramshow, "Tensor viscosity method for convection in numerical fluid dynamics," J. of Compt. Phys., vol. 32, no.1, pp. 71-79, July 1979.
16. R. J. Leveque, Finite difference methods for ordinary and partial differential equations, Society for Industrial and Applied Mathematics, 2007.
17. I. Christie, D. F. Griffiths, A. R. Mitchell, and O. C. Zienkiewicz, "Finite element methods for second order differential equations with significant first derivatives," Int. J. for Num. Methods Eng., vol. 10, no. 6, pp. 1389-1396, 1976.